

# Magnetic quantum tunneling in the half-integer high spin molecule $\text{CrNi}_6$ : a $\mu\text{SR}$ study

A. Keren\*, P. Mendels† A. Kratzer‡, A. Scuille§, M. Verdaguer§, Z. Slaman\* and  
C. Baines¶

*\*Technion-Israel Institute of Technology, Physics Department,*

*Haifa*

*32000, Israel*

*†Laboratoire de Physique des Solides, Bâtiment 510, URA2 CNRS*

*Université*

*Paris Sud, 91405 Orsay, France*

*‡Technische University Physics Department E15, James-Franck-Str,*

*D-85747 Garching, Germany*

*§Laboratoire de Chimie des Métaux de Transition, URA CNRS.*

*419, Université*

*Pierre et Marie Curie, 75252 Paris, France*

*¶Paul Scherrer Institute, CH 5232 Villigen PSI, Switzerland*

(October 20, 2019)

In high spin molecules metal ions are coupled by ferro or antiferromagnetic short range interactions so that their magnetic moments are parallel or antiparallel to each other at temperatures ( $T$ ) much smaller than the coupling constant  $J$ . This leads to a high spin ( $S$ ) value in the ground state. In the crystal lattice, the molecules are well separated from each other and the active part of the Hamiltonian at  $k_B T \ll J$  is  $\mathcal{H} = -DS_z^2$ , so that up and down spins ( $S_z = \pm S$ ) states have identical energies, and  $S_z$  can escape from one state to the other via either over-the-barrier motion, or tunneling. So far[,] the escape rate  $\Gamma$  in HSM was found to have smooth  $T$  dependence throughout the cooling process from  $DS^2 \ll k_B T$  to  $k_B T \ll DS^2$  [1,2]. In this case, the transition from the over-the-barrier

motion to tunneling, is referred to as second-order transition [3]. In the present work, we use the muon spin relaxation technique to show evidence for temperature-independent tunneling at  $k_B T \ll DS^2$ , in zero applied magnetic field (ZF), in the HSM CrNi<sub>6</sub>. Moreover, the crossover from the classical to quantum regime is sharp, and appears to be consistent with a first order transition of the escape rate [3].

In a first order transition, over-the-barrier motion is abruptly replaced by tunneling between ground states, as the temperature is lowered down to the barrier height.

The CrNi<sub>6</sub> molecule is described in details in the methods section. The magnetization  $M$  vs magnetic field  $H$  measured at 6 K in this compound is depicted in Fig. 1.  $M$  displays a saturation value of 15  $\mu_B$ , and fits well to a Brillouin function of  $S = 15/2$ . This  $S$  value is expected from a Cr(III) ( $S_{Cr} = 3/2$ ) ion ferromagnetically coupled to 6 Ni(II) ( $S_{Ni} = 1$ ) ions. The ferromagnetic nature of the interaction is easily rationalized in the frame of a localized electron model, since the quasi-linear Cr-CN-Ni unit allows orthogonality between the Cr(III) and Ni(II) wave functions.

Also shown in Fig. 1 is the thermal variation of the molar susceptibility as the product  $\chi_M T$  vs  $T$ , which monotonously increases from room temperature to 6K. The fit of the measured susceptibility to the one expected from the Hamiltonian  $H = -J \sum_{Ni} \mathbf{S}_{Cr} \cdot \mathbf{S}_{Ni} - DS_z^2$ , shown in this figure, gives a good agreement when choosing a mean  $g$  value = 2, a  $J$  value  $\approx 24$ K, and  $|D| S^2 = 4.2$  K [4]. The value of  $|D| S^2$  is in agreement with ac-susceptibility measurements [5]. The total spin of the molecule ( $S^t = 15/2$ ), is well separated in energy by  $3J/2$  (36K) from an excited level where the total spin  $S^t = 13/2$ , itself  $3J/2$  below a second total spin level where  $S^t = 11/2$ , etc.

The  $\mu$ SR experiments presented here were performed in PSI after preliminary investigation at ISIS using the longitudinal field (LF) technique. In this technique one follows the time evolution of the spin polarization  $P_z(t)$  of a muon implanted in a sample, through the asymmetry  $A(t) \propto P_z(t)$  in the positron emission of the muon decay [6]. In addition, an external field  $H_L$  is applied along the initial muon spin (longitudinal) direction which defines the  $\mathbf{z}$  axis. In view of our experimental results, it is worth discussing the expected behavior

of  $P_z(t)$  in two cases: (I) the field at the muon site is random and static or (II) the field is dynamically fluctuating. In the static case, and when  $H_L = 0$ , the muon polarization relaxes, and the time scale for relaxation  $[\tau]$  is determined by  $(\gamma_\mu[B])^{-1}$  where  $\gamma_\mu = 85.162 \text{ MHz/kG}$  is the muon gyromagnetic ratio and  $[B]$  is the scale of the local magnetic field. However, not all muons will relax since there is a statistical probability that some of them (effectively 1/3) will reside in a site where the field is parallel to the muon spin. Therefore, after a minimum in  $P_z(t)$ , we expect  $\lim_{t \rightarrow \infty} P_z(t) = 1/3$ , a phenomenon called recovery [6]. When the external field is applied, and  $[B] \ll H_L$ , the vector sum of  $H_L$  and the internal field is nearly parallel to the muon spin, and we expect  $\lim_{t \rightarrow \infty} P_z(t) = 1$ . This phenomenaon is called decoupling [6]. In the dynamical case the muon relaxation is determined by the magnetic spectral density at the frequency  $\omega_L = \gamma_\mu H_L$  corresponding to the muon Zeeman energy levels (see below).

In Fig. 2 we show the asymmetry, obtained in  $\text{CrNi}_6$ , in ZF,  $T = 50 \text{ mK}$ , and at various values of  $H_L$ . In the ZF case we find  $\lim_{t \rightarrow \infty} A(t) = 0$ . This limit suggests that the field at the muon site is not static. Moreover, the time scale for the muon relaxation is  $1 \text{ } \mu\text{sec}$ . If this relaxation was due to static fields it would imply a local internal field in the order of tens of Gauss. Such a small field would have decoupled  $[A(t) = A(0)]$  with  $H_L = 2 \text{ kG}$  or higher, in contrast to the observed behavior. We thus conclude that the  $\text{CrNi}_6$  molecules are dynamically fluctuating even at  $T = 50 \text{ mK}$  and in zero applied magnetic field. We interpret[e] these fluctuations as tunneling within the ground spin state, between  $S_z$  levels at the bottom of the anisotropy well, since at  $50 \text{ mK}$  only these levels are populated. A similar conclusion was reached by Vernier *et al.* [7] using high frequency experiments.

In order to illuminate this conclusion we show in the inset of Fig. 2 a similar experiment in a powder of the Ising spin glass  $\text{Fe}_{0.05}\text{TiS}_2$  ( $T_g = 15.5 \text{ K}$ ) at  $T = 4 \text{ K}$  [8]. Here, as in the HSM, the most important degree of freedom is  $S_z$ , and the classical ground state is made of spins randomly oriented in either up or down directions. However, in contrast to  $\text{CrNi}_6$ , we can clearly see in  $\text{Fe}_{0.05}\text{TiS}_2$  a recovery of the asymmetry. In addition, the time scale of muon relaxation in  $\text{Fe}_{0.05}\text{TiS}_2$  is an order of magnitude faster than in  $\text{CrNi}_6$ : yet a field of

720 G is sufficient to nearly fully decouple the muon polarization. Thus,  $\text{Fe}_{0.05}\text{TiS}_2$  fulfills all our expectations from a static magnet and emphasizes in contrast the dynamical nature of  $\text{CrNi}_6$ .

Next we determine the fluctuation rate  $\nu$  (proportional to the escape rate  $\Gamma$ ), where  $\nu$  is defined by  $\langle S(t)S(0) \rangle = \langle S^2 \rangle \exp(-\nu t)$ , and  $S$  is the spin of the ground state of the molecule. Since at low temperatures the spins on the molecule are locked to each other, the fluctuation rate of an individual spin should be identical to that of the entire molecule. Therefore, the relaxation of the muon spin, which is mostly coupled to the electronic spin closest to its stop site, will be determined by  $\nu$ . A second important parameter is the root mean square of the field at the muon site  $\Delta$  ( $= \gamma_\mu \langle B_i^2 \rangle^{1/2}$ ) where  $i$  is a spatial direction. We notice that the muon spin relaxation has a square-root exponential shape, which could be explained by a distribution of  $\Delta$ , due to a distribution of muon sites, according to  $\rho(\Delta) = \sqrt{2/\pi} \frac{a}{\Delta^2} \exp -\frac{a^2}{2\Delta^2}$ . Usually, one can separate the two contributions to the muon relaxation rate by using the LF data. Here the situation is more intricate as the impact of the applied field on the tunneling rate is not evident and in a powder sample  $H_L$  also couples to  $S_x$  and  $S_y$ , and induces tunneling, or to  $S_z$ , and reduces tunneling (for most field values). In the absence of any model, we assume that  $\nu$  is field independent for the fields ( $g\mu_B SH \lesssim DS^2$ ) used here, so as to get an estimate of  $\nu$ . These assumptions lead to

$$A(t) = A_0 \exp \left[ -\sqrt{\frac{4a^2\nu t}{(\omega_L^2 + \nu^2)}} \right] + A_b \quad (1)$$

where,  $A_0$  is the initial asymmetry, and  $A_b$  represent muons that missed the sample [9]. We fit our data to Eq. 1 using  $A_0$ ,  $A_b$ , and  $\nu$ , as global parameters for all data sets. We find reasonable agreement between theory and experiment with a fluctuation rate  $\nu = 85(5)$  MHz and  $a = 10.0(5)$  MHz ( $\sim 100$  G). The fit, shown in Fig. 2 by the solid lines, suggests that indeed the external field might have only minimal impact on the powder averaged tunneling rate at base temperature. One possible explanation for this is that the interaction responsible for tunneling is much stronger than the Zeeman coupling to the external field.

Now we discuss the temperature dependence of the muon relaxation. In Fig. 3 we depict

the muon asymmetry in LF of 100 G and various temperatures; the small field of 100 G is applied in order to decouple the contribution from nuclear moments to the relaxation. We see that from  $T = 50$  to 6 K the muon relaxation rate increases, but between 6 K and 50 mK it remains constant (no change in the asymmetry). The fact that the transition temperature is  $\sim 6$  K reinforces our basic assumption that the electronic spins determine the muon relaxation, since this temperature is of the same order of magnitude as the energy barrier. The  $T$  independent fluctuation rate below  $\sim 6$  K implies that these fluctuations stem from QTM, as opposed to thermally activated, over-the-barrier motion.

We fit the data obtained at different temperatures to Eq. 1, with  $\nu$  the only free parameter, and plot the result in Fig. 4. Clearly, the temperature dependence of  $\nu$  changes abruptly at  $T \sim 10$  K. Also shown in this figure by a solid line is a fit of  $\nu$  to an Arrhenius-like law

$$\nu = \nu_q + \nu_c \exp(-U/T). \quad (2)$$

where  $\nu_q = 85 \mu\text{sec}^{-1}$ . We find  $\nu_c = 12.0(3) \text{ nsec}^{-1}$ , and  $U = 52(3) \text{ K}$ . The large value of  $U$  indicates that for  $T > 10 \text{ K}$  the total spin states  $S^t = 13/2$  and  $S^t = 11/2$ , become populated (recall that  $J_{\text{Ni-Cr}} = 24 \text{ K}$  and that the gap between the lowest total spin states is 36 K). A comparison of Fig. 4 with Fig. 1 suggests that between  $\sim 10 \text{ K}$  and  $\sim 6 \text{ K}$  the molecules condense in a total spin state  $S^t = 15/2$ . The behavior below  $\sim 6 \text{ K}$  suggests that once the temperature becomes as low as the barrier height ( $|D| S^2 = 4.2 \text{ K}$ ), tunneling is taking place between the  $S_z = \pm 15/2$  states; otherwise, it would have shown temperature dependence down to  $\sim D [(15/2)^2 - (13/2)^2] = 1.05 \text{ K}$ . This behaviour appears closely related to a first order quantum-classical transition of the escape rate [3]. It should be pointed out that the nature of the transition is inferred from a nearly zero field experiment and is independent of the absolute value of  $\nu$ , which was determined using the LF.

Our result renders  $\text{CrNi}_6$  the first example of a high spin molecule where the tunneling is temperature independent at low  $T$ , and the transition from the classical activated behavior to the quantum one is sharp and consistent with first order.

## Methods

CrNi<sub>6</sub> -chemical formula [Cr{(CN)Ni(tetren)}<sub>6</sub>](ClO<sub>4</sub>)<sub>9</sub>- is obtained by reacting solutions of 0.1 molar potassium hexacyanochromate(III) and 0.15 molar Ni(II) tetren perchlorate in a mixed solvent water/acetonitrile. The solution is left to evaporate. After a few weeks violet parallelepipedic single crystals appear which are collected, filtered and dried in air. Single crystal X-ray diffraction shows that the compound crystallises in the monoclinic system, P2<sub>1</sub>/n space group, cell parameters  $a = 15.375 \text{ \AA}$ ,  $b = 24.280 \text{ \AA}$ ,  $c = 16.141 \text{ \AA}$ ,  $\alpha = 90^\circ$ ,  $\beta = 115.580^\circ$ ,  $\gamma = 90^\circ$ . Disorder on the perchlorate anions and on the carbon framework of the terminal amine ligands impedes a complete determination of the structure. Nevertheless, it appears clearly that the system is made of heptanuclear entities where the Cr(III) ion is surrounded by six cyanide ions, each bonded to a Ni(II) tetren (see Fig. 1). The coordination sphere of Cr(III) and Ni(II) can be described as a slightly distorted octahedral. The Cr-CN-Ni distance is  $5.23 \text{ \AA}$ . The Cr-CN angle is  $176.02^\circ$ ; the CN-Ni angle is  $170.46^\circ$ . The heptanuclear units are far away from each other (nearest Cr-Cr distance =  $14.77 \text{ \AA}$  and nearest Ni-Ni distance from neighbouring units =  $8.84 \text{ \AA}$ ).

## REFERENCES

- [1] L. Thomas, F. Lioni, R. Ballou, D. Gatteschi, R. Sessoli, and B. Barbara, *Nature* **383**, 145 (1996).
- [2] J. R. Friedman, M. P. Sarachik, J. Tejada, and R. Ziolo, *Phys. Rev. Lett.* **76**, 3830 (1996).
- [3] E. M. Chudnovsky and D. A. Garanin, *Phys. Rev. Lett.* **79**, 4469 (1997).
- [4] T. Mallah, S. Ferlay, A. Sculler, M. Verdaguer, A Rational Molecular Approach to High-Spin Molecules and Molecular Magnets. “Magnetism: A Supramolecular Function” O. Kahn Ed., N.A.T.O. A.S.I. Series C484, Kluwer, Dordrecht, 1996, 597-614
- [5] T. Mallah, C. Auberger, M. Verdaguer, and P. Veillet, *J. Chem. Soc., Chem. Commun.*, 61 (1995).
- [6] P. D. de Réotier and A. Yaouanc, *J. Phys.: Condens. Matter* **9**, 9113 (1997).
- [7] N. Vernier, G. Bellessa, T. Mallah, and M. Verdaguer, *Phys. Rev. B* **56**, 75 (1997).
- [8] F. Gulener *et al.* To be published.
- [9] A. Keren, *Phys. Rev. B* **50**, 10039 (1994).

## Acknowledgements

We should like to thank T. Mallah who first synthesized the compound and for many discussions in the previous steps of the work. We should also like to thank the technical staff of both ISIS and PSI and especially P. J. King and A. Amato for their continu[ous] assistance. We are grateful to E. M Chudnovsky, and G. Bellessa for many suggestions and discussions. These experiments were supported by the European Union through its Training and Mobility of Researchers Program for Large Scale Facilities, and by the Israeli Academy of Science.



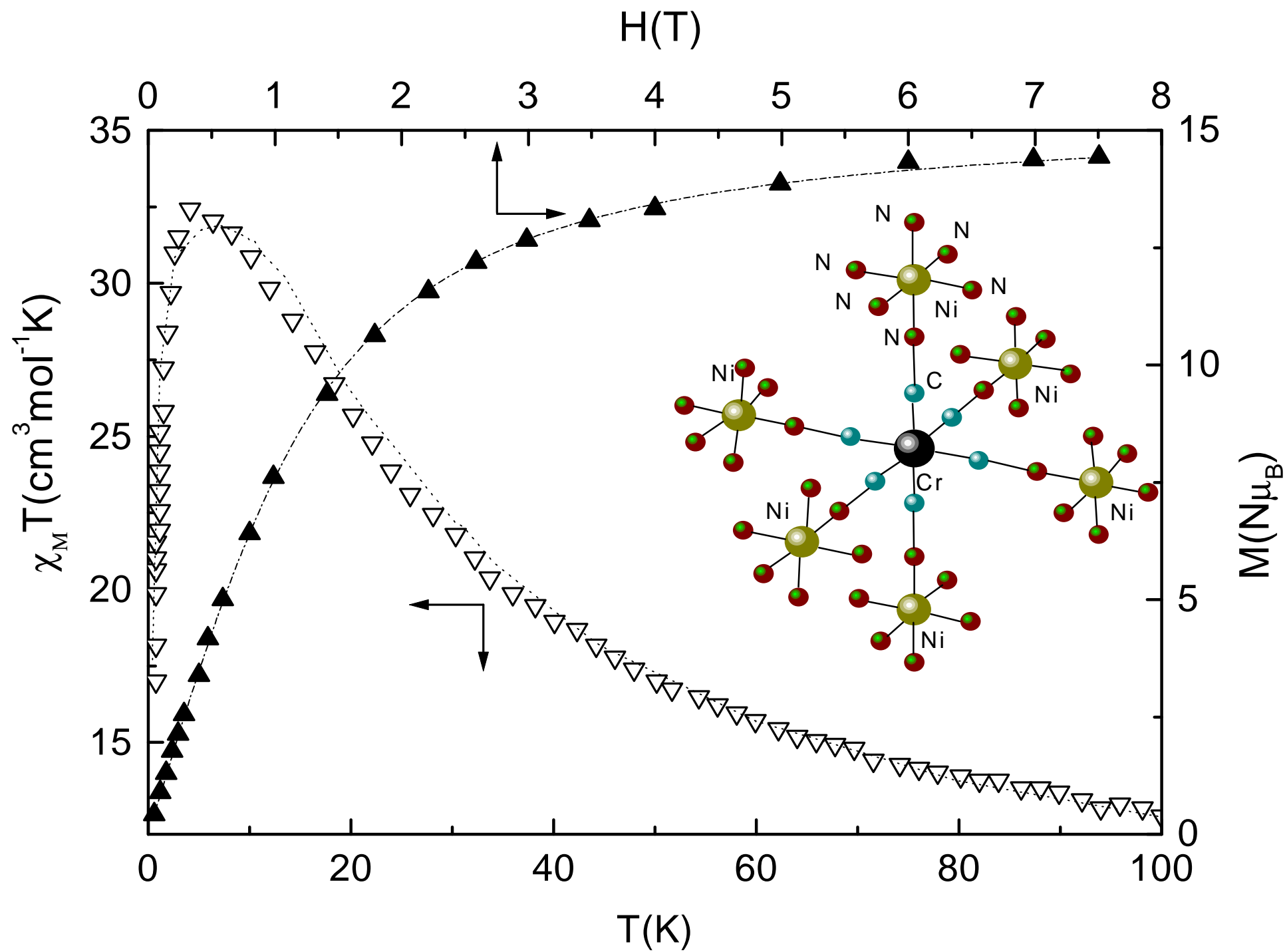
## FIGURES

FIG. 1. Thermal dependence of the molar susceptibility  $\chi_M T$  vs  $T$ , and Magnetis[**z**]ation vs  $H$  at 6K (symbols). The fits (lines) are described in the text. Also shown is the  $\text{CrNi}_6$  molecule.

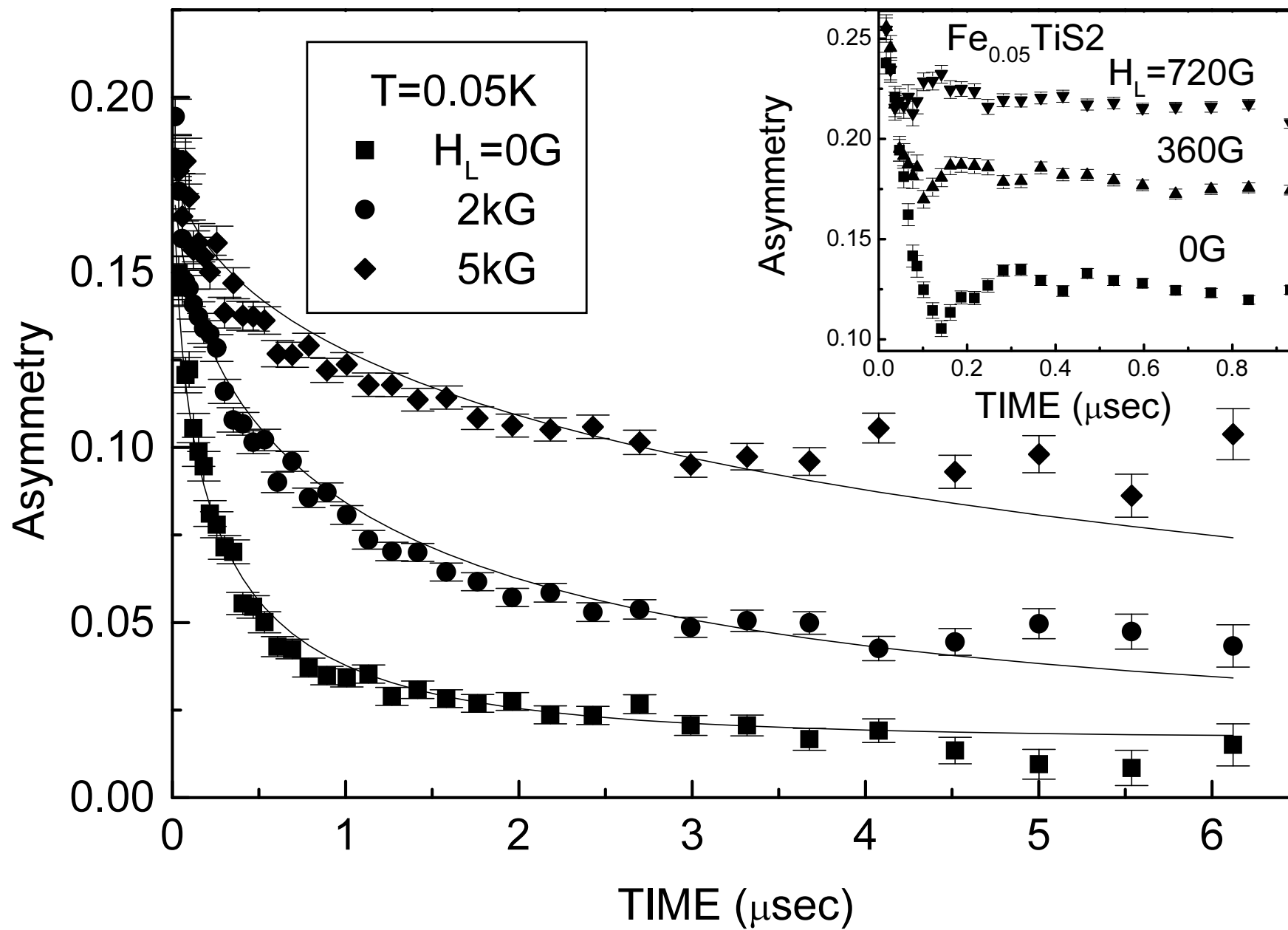
FIG. 2. Muon asymmetry versus time in  $\text{CrNi}_6$  at  $T = 50$  mK and various applied longitudinal magnetic fields. This figure demonstrate[s] the dynamical nature of the electronic spins (see text). For comparison the inset shows the muon asymmetry in the Ising spin glass  $\text{Fe}_{0.05}\text{TiS}_2$  ( $T_g = 15.5$  K) at  $T = 4$  K where these spins are static.

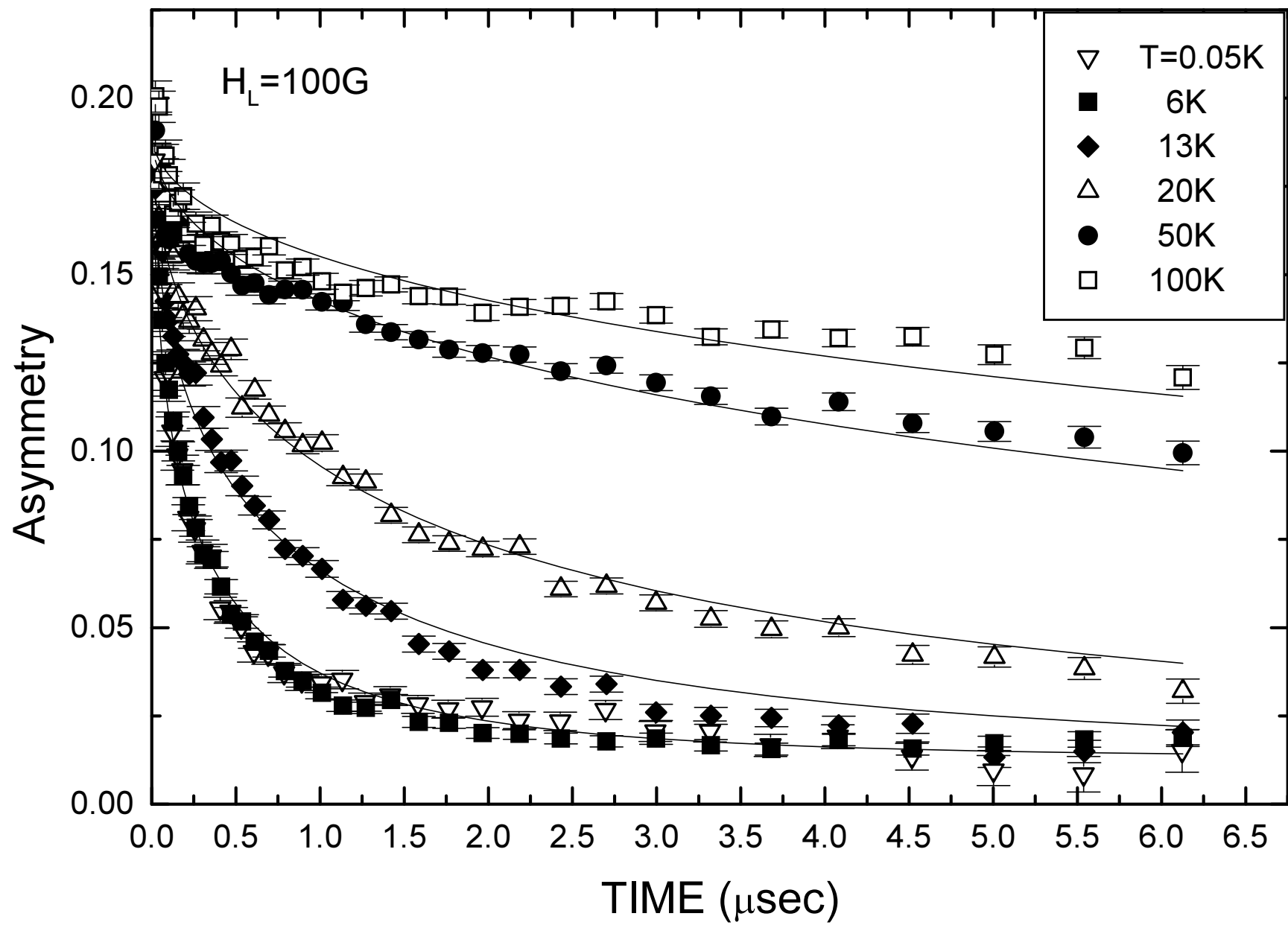
FIG. 3. Muon asymmetry versus time in  $\text{CrNi}_6$  at  $H_L = 100$  G and various temperatures (symbols). The solid line is a fit to Eq. 1.

FIG. 4. Temperature dependence of the molecular spin fluctuation rate. The solid line is a fit to Eq. 2.

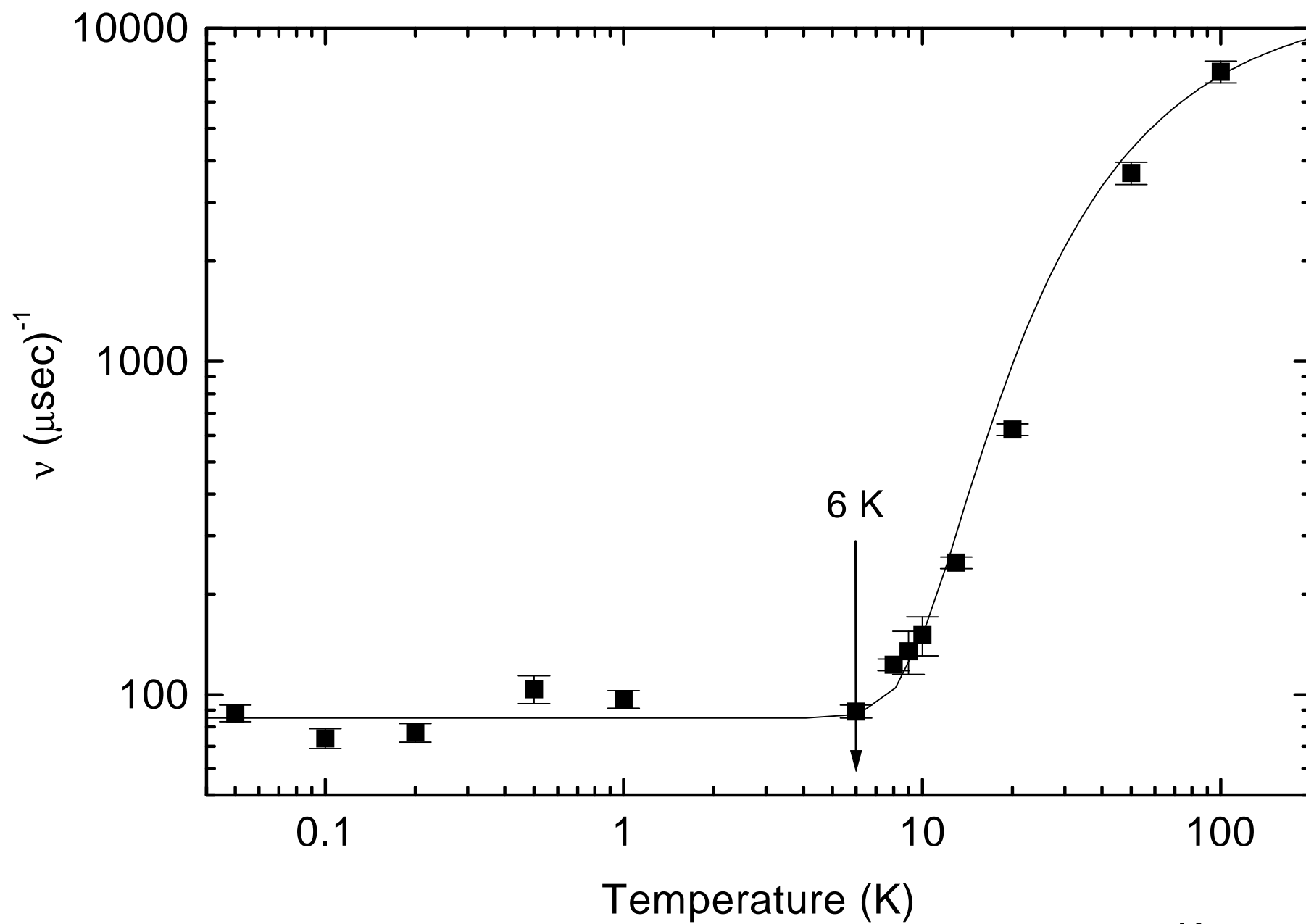


Keren et al. Fig. 1





Keren et al. Fig. 3



Keren et al. Fig. 4